

Multistrange Baryon Elliptic Flow in Au + Au Collisions at $\sqrt{s_{NN}} = 200$ GeV

- J. Adams,³ M. M. Aggarwal,²⁹ Z. Ahammed,⁴³ J. Amonett,²⁰ B. D. Anderson,²⁰ D. Arkhipkin,¹³ G. S. Averichev,¹² S. K. Badyal,¹⁹ Y. Bai,²⁷ J. Balewski,¹⁷ O. Barannikova,³² L. S. Barnby,³ J. Baudot,¹⁸ S. Bekele,²⁸ V. V. Belaga,¹² A. Bellingeri-Laurikainen,³⁸ R. Bellwied,⁴⁶ J. Berger,¹⁴ B. I. Bezverkhny,⁴⁸ S. Bharadwaj,³³ A. Bhasin,¹⁹ A. K. Bhati,²⁹ V. S. Bhatia,²⁹ H. Bichsel,⁴⁵ J. Bielcik,⁴⁸ J. Bielcikova,⁴⁸ A. Billmeier,⁴⁶ L. C. Bland,⁴ C. O. Blyth,³ S. L. Blyth,²¹ B. E. Bonner,³⁴ M. Botje,²⁷ A. Boucham,³⁸ J. Bouchet,³⁸ A. V. Brandin,²⁵ A. Bravar,⁴ M. Bystersky,¹¹ R. V. Cadman,¹ X. Z. Cai,³⁷ H. Caines,⁴⁸ M. Calderón de la Barca Sánchez,¹⁷ J. Castillo,²⁷ O. Catu,⁴⁸ D. Cebra,⁷ Z. Chajecki,²⁸ P. Chaloupka,¹¹ S. Chattopadhyay,⁴³ H. F. Chen,³⁶ J. H. Chen,³⁷ Y. Chen,⁸ J. Cheng,⁴¹ M. Cherney,¹⁰ A. Chikianian,⁴⁸ W. Christie,⁴ J. P. Coffin,¹⁸ T. M. Cormier,⁴⁶ M. R. Cosentino,³⁵ J. G. Cramer,⁴⁵ H. J. Crawford,⁶ D. Das,⁴³ S. Das,⁴³ M. Daugherity,⁴⁰ M. M. de Moura,³⁵ T. G. Dedovich,¹² M. DePhillips,⁴ A. A. Derevschikov,³¹ L. Didenko,⁴ T. Dietel,¹⁴ S. M. Dogra,¹⁹ W. J. Dong,⁸ X. Dong,³⁶ J. E. Draper,⁷ F. Du,⁴⁸ A. K. Dubey,¹⁵ V. B. Dunin,¹² J. C. Dunlop,⁴ M. R. Dutta Mazumdar,⁴³ V. Eckardt,²³ W. R. Edwards,²¹ L. G. Efimov,¹² V. Emelianov,²⁵ J. Engelage,⁶ G. Eppley,³⁴ B. Erasmus,³⁸ M. Estienne,³⁸ P. Fachini,⁴ J. Faivre,¹⁸ R. Fatemi,²² J. Fedorisin,¹² K. Filimonov,²¹ P. Filip,¹¹ E. Finch,⁴⁸ V. Fine,⁴ Y. Fisyak,⁴ K. S. F. Fornazier,³⁵ J. Fu,⁴¹ C. A. Gagliardi,³⁹ L. Gaillard,³ J. Gans,⁴⁸ M. S. Ganti,⁴³ F. Geurts,³⁴ V. Ghazikhanian,⁸ P. Ghosh,⁴³ J. E. Gonzalez,⁸ H. Gos,⁴⁴ O. Grachov,⁴⁶ O. Grebenyuk,²⁷ D. Grosnick,⁴² S. M. Guertin,⁸ Y. Guo,⁴⁶ A. Gupta,¹⁹ N. Gupta,¹⁹ T. D. Gutierrez,⁷ T. J. Hallman,⁴ A. Hamed,⁴⁶ D. Hardtke,²¹ J. W. Harris,⁴⁸ M. Heinz,² T. W. Henry,³⁹ S. Hepplemann,³⁰ B. Hippolyte,¹⁸ A. Hirsch,³² E. Hjort,²¹ G. W. Hoffmann,⁴⁰ M. J. Horner,²¹ H. Z. Huang,⁸ S. L. Huang,³⁶ E. W. Hughes,⁵ T. J. Humanic,²⁸ G. Igo,⁸ A. Ishihara,⁴⁰ P. Jacobs,²¹ W. W. Jacobs,¹⁷ M. Jedynak,⁴⁴ H. Jiang,⁸ P. G. Jones,³ E. G. Judd,⁶ S. Kabana,² K. Kang,⁴¹ M. Kaplan,⁹ D. Keane,²⁰ A. Kechechyan,¹² V. Yu. Khodyrev,³¹ J. Kiryluk,²² A. Kisiel,⁴⁴ E. M. Kislov,¹² J. Klay,²¹ S. R. Klein,²¹ D. D. Koetke,⁴² T. Kollegger,¹⁴ M. Kopytine,²⁰ L. Kotchenda,²⁵ K. L. Kowalik,²¹ M. Kramer,²⁶ P. Kravtsov,²⁵ V. I. Kravtsov,³¹ K. Krueger,¹ C. Kuhn,¹⁸ A. I. Kulikov,¹² A. Kumar,²⁹ R. Kh. Kutuev,¹³ A. A. Kuznetsov,¹² M. A. C. Lamont,⁴⁸ J. M. Landgraf,⁴ S. Lange,¹⁴ F. Laue,⁴ J. Lauret,⁴ A. Lebedev,⁴ R. Lednicky,¹² S. Lehocka,¹² M. J. LeVine,⁴ C. Li,³⁶ Q. Li,⁴⁶ Y. Li,⁴¹ G. Lin,⁴⁸ S. J. Lindenbaum,²⁶ M. A. Lisa,²⁸ F. Liu,⁴⁷ H. Liu,³⁶ J. Liu,³⁴ L. Liu,⁴⁷ Q. J. Liu,⁴⁵ Z. Liu,⁴⁷ T. Ljubicic,⁴ W. J. Llope,³⁴ H. Long,⁸ R. S. Longacre,⁴ M. Lopez-Noriega,²⁸ W. A. Love,⁴ Y. Lu,⁴⁷ T. Ludlam,⁴ D. Lynn,⁴ G. L. Ma,³⁷ J. G. Ma,⁸ Y. G. Ma,³⁷ D. Magestro,²⁸ S. Mahajan,¹⁹ D. P. Mahapatra,¹⁵ R. Majka,⁴⁸ L. K. Mangotra,¹⁹ R. Manweiler,⁴² S. Margetis,²⁰ C. Markert,²⁰ L. Martin,³⁸ J. N. Marx,²¹ H. S. Matis,²¹ Yu. A. Matulenko,³¹ C. J. McClain,¹ T. S. McShane,¹⁰ F. Meissner,²¹ Yu. Melnick,³¹ A. Meschanin,³¹ M. L. Miller,²² N. G. Minaev,³¹ C. Mironov,²⁰ A. Mischke,²⁷ D. K. Mishra,¹⁵ J. Mitchell,³⁴ B. Mohanty,⁴³ L. Molnar,³² C. F. Moore,⁴⁰ D. A. Morozov,³¹ M. G. Munhoz,³⁵ B. K. Nandi,⁴³ S. K. Nayak,¹⁹ T. K. Nayak,⁴³ J. M. Nelson,³ P. K. Netrakanti,⁴³ V. A. Nikitin,¹³ L. V. Nogach,³¹ S. B. Nurushev,³¹ G. Odyniec,²¹ A. Ogawa,⁴ V. Okorokov,²⁵ M. Oldenburg,²¹ D. Olson,²¹ S. K. Pal,⁴³ Y. Panebratsev,¹² S. Y. Panitkin,⁴ A. I. Pavlinov,⁴⁶ T. Pawlak,⁴⁴ T. Peitzmann,²⁷ V. Perevozchikov,⁴ C. Perkins,⁶ W. Peryt,⁴⁴ V. A. Petrov,⁴⁶ S. C. Phatak,¹⁵ R. Picha,⁷ M. Planinic,⁴⁹ J. Pluta,⁴⁴ N. Porile,³² J. Porter,⁴⁵ A. M. Poskanzer,²¹ M. Potekhin,⁴ E. Potrebenikova,¹² B. V. K. S. Potukuchi,¹⁹ D. Prindle,⁴⁵ C. Pruneau,⁴⁶ J. Putschke,²¹ G. Rakness,³⁰ R. Raniwala,³³ S. Raniwala,³³ O. Ravel,³⁸ R. L. Ray,⁴⁰ S. V. Razin,¹² D. Reichhold,³² J. G. Reid,⁴⁵ J. Reinnarth,³⁸ G. Renault,³⁸ F. Retiere,²¹ A. Ridiger,²⁵ H. G. Ritter,²¹ J. B. Roberts,³⁴ O. V. Rogachevskiy,¹² J. L. Romero,⁷ A. Rose,²¹ C. Roy,³⁸ L. Ruan,³⁶ M. Russcher,²⁷ R. Sahoo,¹⁵ I. Sakrejda,²¹ S. Salur,⁴⁸ J. Sandweiss,⁴⁸ M. Sarsour,¹⁷ I. Savin,¹³ P. S. Sazhin,¹² J. Schambach,⁴⁰ R. P. Scharenberg,³² N. Schmitz,²³ K. Schweda,²¹ J. Seger,¹⁰ P. Seyboth,²³ E. Shahaliev,¹² M. Shao,³⁶ W. Shao,⁵ M. Sharma,²⁹ W. Q. Shen,³⁷ K. E. Shestermanov,³¹ S. S. Shimanskiy,¹² E. Sichtermann,²¹ F. Simon,²² R. N. Singaraju,⁴³ N. Smirnov,⁴⁸ R. Snellings,²⁷ G. Sood,⁴² P. Sorensen,²¹ J. Sowinski,¹⁷ J. Speltz,¹⁸ H. M. Spinka,¹ B. Srivastava,³² A. Stadnik,¹² T. D. S. Stanislaus,⁴² R. Stock,¹⁴ A. Stolpovsky,⁴⁶ M. Strikhanov,²⁵ B. Stringfellow,³² A. A. P. Suaide,³⁵ E. Sugarbaker,²⁸ C. Suire,⁴ M. Sumbera,¹¹ B. Surrow,²² M. Swanger,¹⁰ T. J. M. Symons,²¹ A. Szanto de Toledo,³⁵ A. Tai,⁸ J. Takahashi,³⁵ A. H. Tang,²⁷ T. Tarnowsky,³² D. Thein,⁸ J. H. Thomas,²¹ A. R. Timmins,³ S. Timoshenko,²⁵ M. Tokarev,¹² S. Trentalange,⁸ R. E. Tribble,³⁹ O. D. Tsai,⁸ J. Ulery,³² T. Ullrich,⁴ D. G. Underwood,¹ G. Van Buren,⁴ N. van der Kolk,²⁷ M. van Leeuwen,²¹ A. M. Vander Molen,²⁴ R. Varma,¹⁶ I. M. Vasilevski,¹³ A. N. Vasiliev,³¹ R. Vernet,¹⁸ S. E. Vigdor,¹⁷ Y. P. Viyogi,⁴³ S. Vokal,¹² S. A. Voloshin,⁴⁶ W. T. Waggoner,¹⁰ F. Wang,³² G. Wang,²⁰ G. Wang,⁵ X. L. Wang,³⁶ Y. Wang,⁴⁰ Y. Wang,⁴¹ Z. M. Wang,³⁶ H. Ward,⁴⁰ J. W. Watson,²⁰ J. C. Webb,¹⁷ G. D. Westfall,²⁴ A. Wetzler,²¹ C. Whitten, Jr.,⁸ H. Wieman,²¹ S. W. Wissink,¹⁷ R. Witt,² J. Wood,⁸ J. Wu,³⁶ N. Xu,²¹ Z. Xu,⁴ Z. Z. Xu,³⁶ E. Yamamoto,²¹ P. Yepes,³⁴

V.I. Yurevich,¹² I. Zborovsky,¹¹ H. Zhang,⁴ W.M. Zhang,²⁰ Y. Zhang,³⁶ Z. P. Zhang,³⁶ C. Zhong,³⁷ R. Zoukarneev,¹³
Y. Zoukarneeva,¹³ A.N. Zubarev,¹² and J.X. Zuo³⁷

(STAR Collaboration)

¹Argonne National Laboratory, Argonne, Illinois 60439, USA

²University of Bern, 3012 Bern, Switzerland

³University of Birmingham, Birmingham, United Kingdom

⁴Brookhaven National Laboratory, Upton, New York 11973, USA

⁵California Institute of Technology, Pasadena, California 91125, USA

⁶University of California, Berkeley, California 94720, USA

⁷University of California, Davis, California 95616, USA

⁸University of California, Los Angeles, California 90095, USA

⁹Carnegie Mellon University, Pittsburgh, Pennsylvania 15213, USA

¹⁰Creighton University, Omaha, Nebraska 68178, USA

¹¹Nuclear Physics Institute AS CR, 25068 Řež/Prague, Czech Republic

¹²Laboratory for High Energy (JINR), Dubna, Russia

¹³Particle Physics Laboratory (JINR), Dubna, Russia

¹⁴University of Frankfurt, Frankfurt, Germany

¹⁵Institute of Physics, Bhubaneswar 751005, India

¹⁶Indian Institute of Technology, Mumbai, India

¹⁷Indiana University, Bloomington, Indiana 47408, USA

¹⁸Institut de Recherches Subatomiques, Strasbourg, France

¹⁹University of Jammu, Jammu 180001, India

²⁰Kent State University, Kent, Ohio 44242, USA

²¹Lawrence Berkeley National Laboratory, Berkeley, California 94720, USA

²²Massachusetts Institute of Technology, Cambridge, Massachusetts 02139-4307, USA

²³Max-Planck-Institut für Physik, Munich, Germany

²⁴Michigan State University, East Lansing, Michigan 48824, USA

²⁵Moscow Engineering Physics Institute, Moscow, Russia

²⁶City College of New York, New York, New York 10031, USA

²⁷NIKHEF and Utrecht University, Amsterdam, The Netherlands

²⁸Ohio State University, Columbus, Ohio 43210, USA

²⁹Panjab University, Chandigarh 160014, India

³⁰Pennsylvania State University, University Park, Pennsylvania 16802, USA

³¹Institute of High Energy Physics, Protvino, Russia

³²Purdue University, West Lafayette, Indiana 47907, USA

³³University of Rajasthan, Jaipur 302004, India

³⁴Rice University, Houston, Texas 77251, USA

³⁵Universidade de São Paulo, São Paulo, Brazil

³⁶University of Science and Technology of China, Anhui 230027, China

³⁷Shanghai Institute of Applied Physics, Shanghai 201800, China

³⁸SUBATECH, Nantes, France

³⁹Texas A&M University, College Station, Texas 77843, USA

⁴⁰University of Texas, Austin, Texas 78712, USA

⁴¹Tsinghua University, Beijing 100084, China

⁴²Valparaiso University, Valparaiso, Indiana 46383, USA

⁴³Variable Energy Cyclotron Centre, Kolkata 700064, India

⁴⁴Warsaw University of Technology, Warsaw, Poland

⁴⁵University of Washington, Seattle, Washington 98195, USA

⁴⁶Wayne State University, Detroit, Michigan 48201, USA

⁴⁷Institute of Particle Physics, CCNU (HZNU), Wuhan 430079, China

⁴⁸Yale University, New Haven, Connecticut 06520, USA

⁴⁹University of Zagreb, Zagreb HR-10002, Croatia

(Received 22 April 2005; published 13 September 2005)

We report on the first measurement of elliptic flow $v_2(p_T)$ of multistrange baryons $\Xi^- + \bar{\Xi}^{++}$ and $\Omega^- + \bar{\Omega}^{++}$ in heavy-ion collisions. In minimum-bias Au + Au collisions at $\sqrt{s_{NN}} = 200$ GeV, a significant amount of elliptic flow, comparable to other nonstrange baryons, is observed for multistrange baryons which are expected to be particularly sensitive to the dynamics of the partonic stage of heavy-ion collisions. The p_T dependence of v_2 of the multistrange baryons confirms the number of constituent quark

scaling previously observed for lighter hadrons. These results support the idea that a substantial fraction of the observed collective motion is developed at the early partonic stage in ultrarelativistic nuclear collisions at the Relativistic Heavy Ion Collider.

DOI: 10.1103/PhysRevLett.95.122301

PACS numbers: 25.75.Ld

Lattice QCD calculations, at vanishing or finite net-baryon density, predict a transition from the deconfined thermalized partonic matter quark gluon plasma to ordinary hadronic matter at a critical temperature $T_{c\psi} \approx 150$ – 180 MeV [1,2]. Measurements of hadron yields in the intermediate ($2 \leq p_{T\psi} \leq 6$ GeV/ c) and high ($p_{T\psi} \geq 6$ – 8 GeV/ c) transverse momentum $p_{T\psi}$ region indicate that dense matter has been produced in Au + Au collisions at the Relativistic Heavy Ion Collider (RHIC) [3–10]. Furthermore, previous measurements of elliptic flow of hadrons indicate that the matter created at RHIC is also strongly interacting [11,12]. Thus, in the early stage of the collision, dense and strongly interacting matter will lead to collective effects among constituents such as transverse collective motion. If these interactions occur frequently enough, the system will then reach thermalization. Because of the initial spatial anisotropy of the system in noncentral collisions, an elliptic component of the collective transverse motion should also be present. Collectivity is cumulative throughout the whole collision and should survive the hadronization process [13,14]; therefore, the amount of transverse flow observed in the final state will have a contribution from the prehadronic, i.e., partonic, stage.

Early dynamic information might be masked by later hadronic rescatterings. Multistrange baryons with their large mass and presumably small hadronic cross sections [15–19] should be less sensitive to hadronic rescattering in the later stages of the collision and therefore a good probe of the early stage of the collision [20]. Indeed, a systematic study of hadron $p_{T\psi}$ spectra from high-energy heavy-ion collisions, using a hydrodynamically inspired model, shows that multistrange baryons thermally freeze-out close to the point where chemical freeze-out occurs with $T_{ch} \sim 160$ MeV [20,21], which at these collision energies coincides with the critical temperature $T_{c\psi}$ [1,2]. This may mean that multistrange baryons are not, or much less, affected by hadronic rescatterings during the later stage of heavy-ion collisions [15,16]. Their observed transverse flow would then primarily reflect the partonic flow. Moreover, elliptic flow is in itself considered to be a good tool for understanding the properties of the early stage of the collisions [22,23], primarily due to its self-quenching nature. Elliptic flow is generated from the initial spatial anisotropy of the system created in noncentral collisions by rescatterings among the constituents of the system. The generated elliptic flow will reduce the spatial anisotropy of the system and quench its own origin. Thus multistrange baryon elliptic flow could be a valuable probe of the initial partonic system.

In this Letter, we present the first results on elliptic flow of multistrange baryons $\Xi^- + \bar{\Xi}^+$ and $\Omega^- + \bar{\Omega}^+$ from Au + Au collisions at $\sqrt{s_{NN\psi}} = 200$ GeV, as measured with the STAR detector [24]. About 2×10^6 events from Au + Au collisions collected with a minimum-bias trigger are used in this analysis. Multistrange baryons are reconstructed via their decay topology: $\Xi \rightarrow A + \pi\psi$ and $\Omega \rightarrow \Lambda + K\psi$ with the subsequent decay of $\Lambda \rightarrow p + \pi\psi$ as described in [20]. Charged tracks were reconstructed in the STAR time projection chamber [25]. Simple cuts on geometry, kinematics, and particle identification via specific ionization are applied to reduce the combinatorial background. A detailed description of the analysis procedure can be found in [20,26].

Figure 1 shows the invariant mass distribution for (a) $\Xi^- + \bar{\Xi}^+$ and (b) $\Omega^- + \bar{\Omega}^+$ candidates from minimum-bias collisions (0%–80% of the total hadronic cross section). The $\Xi^- + \bar{\Xi}^+$ and $\Omega^- + \bar{\Omega}^+$ signals appear as clear peaks around the rest masses (indicated by the vertical arrows) in the invariant mass distribution, above a combinatorial background. The combinatorial background of uncorrelated decay candidates under the peak can be

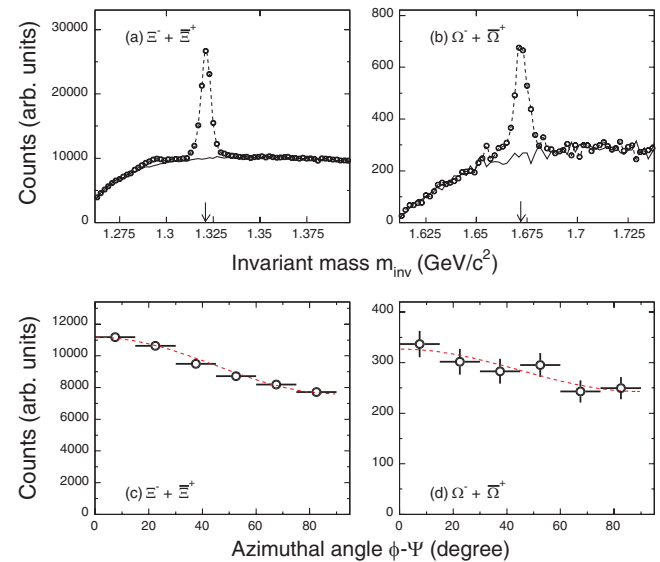


FIG. 1 (color online). (a) $\Xi^- + \bar{\Xi}^+$ and (b) $\Omega^- + \bar{\Omega}^+$ invariant mass distribution from minimum-bias (0%–80%) Au + Au collisions at $\sqrt{s_{NN\psi}} = 200$ GeV. The solid lines show the combinatorial background as estimated from a same event rotating method (see text for details). Azimuthal distributions with respect to the event plane of the (c) $\Xi^- + \bar{\Xi}^+$ and (d) $\Omega^- + \bar{\Omega}^+$ raw yields. Dashed lines represent the fit results. All plots shown include $\Xi^- + \bar{\Xi}^+$ and $\Omega^- + \bar{\Omega}^+$ in the transverse momentum range $1 < p_{T\psi} < 4$ GeV/ c .

determined by sampling the regions on both sides of the peak. It can also be reproduced by rotating the Λ candidates by 180° in the transverse plane and then reconstructing the Ξ and Ω candidates. The rotation of the Λ breaks the correlation in the invariant mass and therefore mimics the background of uncorrelated decay pairs. Both background determination methods provide consistent results. In Figs. 1(a) and 1(b), the combinatorial background as calculated from the rotation method is shown as solid lines. Outside the region of the corresponding mass peak, the rotation method describes the background well. The residual *bump* at lower invariant mass than the peak in Fig. 1(a) can be understood as fake Ξ candidates being reconstructed as $\Xi_{\text{fake}}(\pi_\Lambda, \Lambda_{\text{fake}}(\pi_{\text{random}}, p_\Lambda))$, where π_Λ and p_Λ are the daughters of a real Λ and π_{random} is a random π . The real correlation between π_Λ and p_Λ remains in the Ξ_{fake} reconstruction resulting in the observed bump in the Ξ invariant mass distribution. A similar misassociation happens in the Ω case with the addition of the π_Λ being misidentified as a kaon. Our studies have shown that this residual correlation does not affect the signal peak. The raw yields are then extracted from the invariant mass distribution by counting the number of entries in the mass peak above the estimated background.

The elliptic flow ν_2 is calculated from the distribution of particle raw yields as a function of azimuthal angle ϕ with respect to the event plane angle Ψ . The Ξ and Ω candidates are divided in $\phi \psi - \Psi$ bins, and the raw yields for each bin are extracted from the invariant mass distributions as described above. The event plane angle Ψ is used as an estimate of the reaction plane angle [27,28]. Here, the event plane is determined from the azimuthal distribution of charged primary tracks with $0.2 < p_{T\psi} < 4.0$ GeV/c and pseudorapidity $|\eta| < 1.0$. To avoid autocorrelations, tracks associated with a Ξ or an Ω candidate are explicitly excluded from the event plane calculation. Figure 1 shows the azimuthal distributions of raw yields for (c) $\Xi^- + \bar{\Xi}^+$ and (d) $\Omega^- + \bar{\Omega}^+$ with respect to the event plane from the minimum-bias collisions in the $1 < p_{T\psi} < 4$ GeV/c range. To reduce the statistical uncertainties in the Ξ and Ω signal extraction and because of the $\cos 2(\phi - \Psi)$ dependence of ν_2 , we have folded around $\pi/2$ the candidates in the $\pi/2 < \phi \psi - \Psi < \pi$ range into the $\pi/2 > \phi \psi - \Psi > 0$ range. The distributions exhibit a clear oscillation with azimuthal angle $\phi - \Psi$ for both Ξ and Ω particles, indicating the presence of significant elliptic flow. The dashed lines are the results from fitting a function $\frac{dN_d}{d(\phi - \Psi)} = A[1 + 2\nu_2 \cos 2(\phi - \Psi)]$, where A is the normalization constant. Furthermore, we note that the amplitude of the oscillation for the Ξ and Ω are of similar magnitude, indicating that their ν_2 is similar, as will be discussed later. The finite resolution in the event plane determination smears out the azimuthal distributions and leads to a lower signal in the apparent anisotropy [28]. We determine the event plane resolution by dividing each event into random subevents and determine the correction factor to be 1/0.72

for minimum-bias collisions. In the following, all numbers reported on ν_2 are corrected for this resolution. Systematic uncertainties in ν_2 were studied by comparing the background determination methods described above and by changing the cuts used in the Ξ and Ω reconstruction. For the Ξ , the estimated absolute systematic uncertainties are 0.02 for the lowest $p_{T\psi}$ bin and smaller than 0.01 for all other $p_{T\psi}$ bins. For the Ω , the absolute systematic uncertainty is 0.04 for both measured transverse momentum bins. Correlations unrelated to the reaction plane (nonflow effects) can modify the apparent ν_2 [11]. Nonflow contributions for multistrange baryons have not been studied yet, but are expected to be similar to those calculated for Λ (~ -0.01 at $p_{T\psi} = 4$ GeV/c and ~ -0.04 at $p_{T\psi} = 2.5$ and 4.0 GeV/c) [11].

Figure 2 shows the results of the elliptic flow parameter $\nu_2(p_T)$ for multistrange baryons (a) $\Xi^- + \bar{\Xi}^+$ and (b) $\Omega^- + \bar{\Omega}^+$ from minimum-bias (0%–80%) Au + Au collisions. As a reference, the open symbols represent the published [11] K_S^0 and Λ $\nu_2(p_t)$ from the same event class. As a guideline, results of the fit [29] to $\nu_2(p_T)$ of K_S^0 and Λ are shown as dashed lines. Hydrodynamic model calcula-

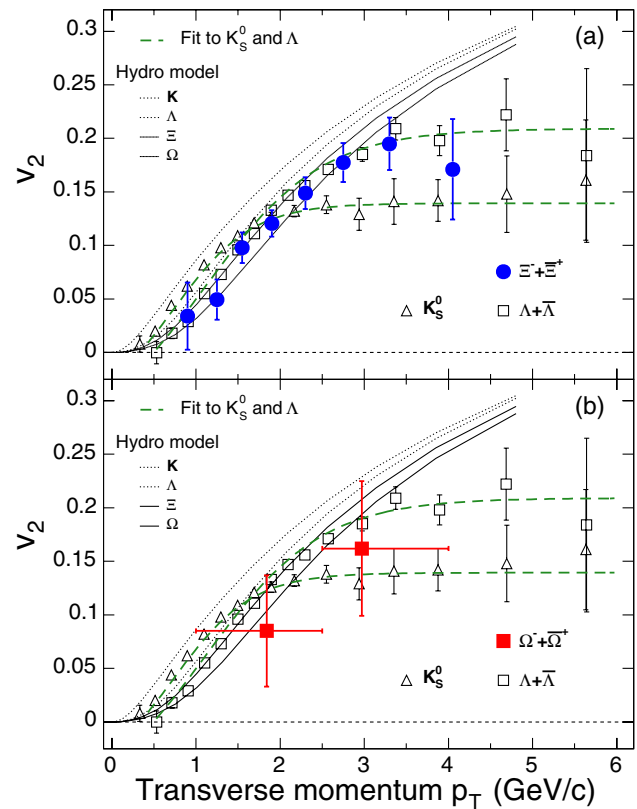


FIG. 2 (color online). $\nu_2(p_T)$ of (a) $\Xi^- + \bar{\Xi}^+$ and (b) $\Omega^- + \bar{\Omega}^+$ from 200 GeV Au + Au minimum-bias collisions. The ν_2 of K_S^0 and Λ [11] are also shown as open symbols, and the results of the fits [29] are shown as dashed lines. Hydrodynamic model calculations [30] are shown as dotted lines for K and Λ and as solid lines for Ξ^- and Ω^- masses, from top to bottom, respectively.

tions using an equation of state with a phase transition at $T_{c\psi} = 465$ MeV and a thermal freeze-out at T_{fo} 130 MeV [30] are shown as dotted lines for $K\psi$ and Λ and as solid lines for Ξ and Ω , from top to bottom, respectively. The expected mass ordering in hydrodynamics of $\nu_2(p_T)$ is observed with lighter particles having larger $\nu_2(p_T)$ than heavier particles. We note that, in this hydrodynamic model calculation, a significant fraction of the elliptic flow is generated prior to the phase transition.

First, we observe in Fig. 2(a) that for Ξ the ν_2 increases with p_T , reaching a saturation value of 18% at $p_{T\psi} = 3.0$ GeV/c. This is similar to the result for Λ baryons [11]. In the lower p_T region ($p_{T\psi} < 2.5$ GeV/c), the Ξ results are in agreement with the hydrodynamic model prediction [30]. In the intermediate p_T region, however, the Ξ results start to deviate (as expected) from the hydrodynamic model prediction, as do the Λ . Second, we observe in Fig. 2(b) that the values of ν_2 for the Ω are clearly non-vanishing although they have larger statistical uncertainties due to their smaller abundance. Over the measured $p_{T\psi}$ range and considering the statistical uncertainties, the ν_2 of the Ω is nonzero with 99.73% confidence level (3σ) effect). The Ω ν_2 values are, within uncertainties, consistent with those measured for the Ξ , indicating that even the triply strange baryon Ω has developed significant elliptic flow in Au + Au collisions at RHIC. In the scenario where multistrange baryons are less affected by the hadronic stage [20] and where ν_2 develops primarily at the early stage of the collision [22,23], the large ν_2 of multistrange baryons reported in this Letter shows that partonic collectivity is generated at RHIC.

Previously, a particle type (baryon versus meson) difference in $\nu_2(p_t)$ was observed for π^+ and $p\bar{p}$ [31] as well as for $K_{S\psi}^0$ and Λ [11] at the intermediate $p_{T\psi}$ region. The present results on the Ξ $\nu_2(p_t)$ follow closely the ones for Λ , confirming that this observed particle type difference, in the intermediate $p_{T\psi}$ region, is a meson-baryon effect rather than a mass effect. This particle type dependence of the $\nu_2(p_T)$ is naturally accounted for by quark coalescence or recombination models [32–34]. In these hadronization models, hadrons are formed dominantly by coalescing massive quarks from a partonic system with the underlying assumption of collectivity among these quarks. Should there be no difference in collectivity among u , d , and s quarks near hadronization, these models predict a universal scaling of ν_2 and the hadron transverse momentum $p_{T\psi}$ with the number of constituent quarks (n_q). This scaling has previously been observed to hold within experimental uncertainties for the $K_{S\psi}^0$ and the Λ when $p_T/n_q \geq 0.7$ GeV/c [11].

The n_q -scaled ν_2 versus the n_q -scaled $p_{T\psi}$ are shown in Fig. 3 for $\pi^- + \pi^+$ (open diamonds), $p\bar{p}$ (open circles) [31], $K_{S\psi}^0$ (open triangles), $\Lambda + \bar{\Lambda}$ (open squares) [11], $\Xi^- + \Xi^+$ (solid circles), and $\Omega^- + \bar{\Omega}^+$ (solid squares). Except for pions, all hadrons, including Ξ and Ω , scale well within statistics. The discrepancy in the pion ν_2 may

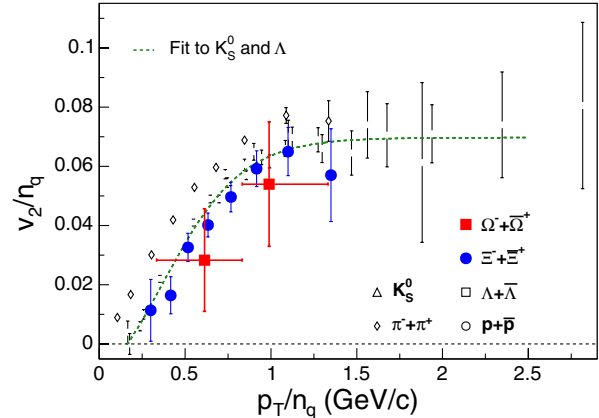


FIG. 3 (color online). Number of quark (n_q) scaled ν_2 as a function of scaled $p_{T\psi}$ for $\Xi^- + \Xi^+$ (solid circles) and $\Omega^- + \bar{\Omega}^+$ (solid squares). Same distributions also shown for $\pi^+ + \pi^-$ (open diamonds), $p\bar{p}$ (open triangles) [31], $K_{S\psi}^0$ (open circles), and $\Lambda + \bar{\Lambda}$ (open squares) [11]. All data are from 200 GeV Au + Au minimum-bias collisions. The dashed line is the scaled result of the fit to $K_{S\psi}^0$ and Λ [29].

in part be attributed to its Goldstone boson nature (its mass is smaller than the sum of its constituent quark masses) or to the effects of resonance decays (a large fraction of the measured pions will come from the decays of resonances at higher p_T) [29,35]. This further success of the coalescence models in describing the multistrange baryon $\nu_2(p_T)$ also lends strong support to the finding that collectivity developed in the partonic stage at RHIC. In addition, the good agreement of $\nu_2(p_T/n_q)/n_q$ for $p(uud)$, $\Lambda(uds)$, $\Xi(dss)$, and $\Omega(sss)$ further supports the idea that the partonic flow of s quarks is similar to that of u , d quarks. Future measurements with higher statistics, specially for the Ω , will allow for a more quantitative comparison.

In summary, we reported the STAR results on multistrange baryon, $\Xi^- + \Xi^+$ and $\Omega^- + \bar{\Omega}^+$, elliptic flow ν_2 from minimum-bias Au + Au collisions at $\sqrt{s_{NN}} = 200$ GeV. The observations of sizable elliptic flow and the constituent quark scaling behavior for the multistrange baryons suggest that substantial collective motion has been developed prior to hadronization in the high-energy nuclear collisions at RHIC.

We thank the RHIC Operations Group and RCF at BNL, and the NERSC Center at LBNL for their support. This work was supported in part by the HENP Divisions of the Office of Science of the U.S. DOE; the U.S. NSF; the BMBF of Germany; IN2P3, RA, RPL, and EMN of France; EPSRC of the United Kingdom; FAPESP of Brazil; the Russian Ministry of Science and Technology; the Ministry of Education and the NNSFC of China; IRP and GA of the Czech Republic; FOM of the Netherlands; DAE, DST, and CSIR of the Government of India; Swiss NSF; the Polish State Committee for Scientific Research; and the STAA of Slovakia.

- [1] F. Karsch, Nucl. Phys. **A698**, 199c (2002).
- [2] Z. Fodor, Nucl. Phys. **A715**, 319c (2003), and references therein; Z. Fodor and S. D. Katz, Phys. Lett. B **534**, 87 (2002).
- [3] C. Adler *et al.* (STAR Collaboration), Phys. Rev. Lett. **89**, 202301 (2002).
- [4] J. Adam *et al.* (STAR Collaboration), Phys. Rev. Lett. **91**, 172302 (2003).
- [5] J. Adam *et al.* (STAR Collaboration), Phys. Rev. Lett. **91**, 072304 (2003).
- [6] K. Adcox *et al.* (PHENIX Collaboration), Phys. Rev. Lett. **88**, 022301 (2002).
- [7] S. S. Adler *et al.* (PHENIX Collaboration), Phys. Rev. Lett. **91**, 072301 (2003).
- [8] S. S. Adler *et al.* (PHENIX Collaboration), Phys. Rev. Lett. **91**, 072303 (2003).
- [9] B. B. Back *et al.* (PHOBOS Collaboration), Phys. Rev. Lett. **91**, 072302 (2003).
- [10] I. Arsene *et al.* (BRAHMS Collaboration), Phys. Rev. Lett. **91**, 072305 (2003).
- [11] J. Adam *et al.* (STAR Collaboration), Phys. Rev. Lett. **92**, 052302 (2004).
- [12] C. Adler *et al.* (STAR Collaboration), Phys. Rev. Lett. **87**, 182301 (2001).
- [13] P. F. Kolb and U. Heinz, nucl-th/0305084.
- [14] D. Teaney, J. Lauret, and E. V. Shuryak, nucl-th/0110037.
- [15] H. van Hecke, H. Sorge, and N. Xu, Phys. Rev. Lett. **81**, 5764 (1998).
- [16] S. A. Bass *et al.*, Phys. Rev. C **60**, 021902 (1999); A. Dumitru, S. A. Bass, M. Bleicher, H. Stöcker, and W. Greiner, Phys. Lett. B **460**, 411 (1999); S. A. Bass and A. Dumitru, Phys. Rev. C **61**, 064909 (2000).
- [17] Y. Cheng *et al.*, Phys. Rev. C **68**, 034910 (2003).
- [18] S. F. Biagi *et al.*, Nucl. Phys. **B186**, 1 (1981).
- [19] R. A. Muller, Phys. Lett. **38B**, 123 (1972).
- [20] J. Adam *et al.* (STAR Collaboration), Phys. Rev. Lett. **92**, 182301 (2004).
- [21] C. Alt *et al.* (NA49 Collaboration), Phys. Rev. Lett. **94**, 192301 (2005).
- [22] H. Sorge, Phys. Rev. Lett. **82**, 2048 (1999).
- [23] J. Y. Ollitrault, Phys. Rev. D **46**, 229 (1992).
- [24] K. H. Ackermann *et al.* (STAR Collaboration), Nucl. Instrum. Methods Phys. Res., Sect. A **499**, 624 (2003).
- [25] M. Anderson *et al.*, Nucl. Instrum. Methods Phys. Res., Sect. A **499**, 659 (2003).
- [26] C. Adler *et al.* (STAR Collaboration), Phys. Rev. Lett. **89**, 092301 (2002).
- [27] K. H. Ackermann *et al.* (STAR Collaboration), Phys. Rev. Lett. **86**, 402 (2001).
- [28] A. Poskanzer and S. A. Voloshin, Phys. Rev. C **58**, 1671 (1998).
- [29] X. Dong, S. Esumi, P. Sorensen, N. Xu, and Z. Xu, Phys. Lett. B **597**, 328 (2004).
- [30] P. Huovinen (private communication); P. Huovinen, P. F. Kolb, U. Heinz, P. V. Ruuskanen, and S. Voloshin, Phys. Lett. B **503**, 58 (2001).
- [31] S. S. Adler *et al.* (PHENIX Collaboration), Phys. Rev. Lett. **91**, 182301 (2003).
- [32] S. Voloshin, Nucl. Phys. **A715**, 379c (2003); D. Molnar and S. Voloshin, Phys. Rev. Lett. **91**, 092301 (2003).
- [33] R. J. Fries, B. Müller, C. Nonaka, and S. A. Bass, Phys. Rev. Lett. **90**, 202303 (2003).
- [34] Z. Lin and C. Ko, Phys. Rev. Lett. **89**, 202302 (2002).
- [35] V. Greco and C. Ko, Phys. Rev. C **70**, 024901 (2004).